analytical chemistry

Article

pubs.acs.org/ac

Highly Sensitive Multiple microRNA Detection Based on Fluorescence Quenching of Graphene Oxide and Isothermal Strand-Displacement Polymerase Reaction

Haifeng Dong,[†] Jing Zhang,[‡,§] Huangxian Ju,*[,§] Huiting Lu,[†] Shiyan Wang,[†] Shi Jin,[†] Kaihong Hao,[†] Hongwu Du,[†] and Xueji Zhang*[,†]

[†]Research Center for Bioengineering and Sensing Technology, University of Science & Technology Beijing, Beijing 100083, P.R. China

[‡]School of Petrochemical Engineering, Changzhou University, Changzhou 213164, P.R. China

[§]State Key Laboratory of Analytical Chemistry for Life Science, Department of Chemistry and Chemical Engineering, Nanjing University, Nanjing 210093, P.R. China

ABSTRACT: A simple, highly sensitive, and selective multiple microRNA (miRNA) detection method based on the graphene oxide (GO) fluorescence quenching and isothermal strand-displacement polymerase reaction (ISDPR) was proposed. The capability to discriminate ssDNA and double-stranded nucleic acid structure coupled with the extraordinary fluorescence quenching of GO on multiple organic dye allows the proposed strategy to simultaneously and selectively detect several miRNA labeled with different dyes in the same solution, while the ISDPR amplification endows the detection method with high sensitivity. The strong interaction between ssDNA and GO led to the fluorescent ssDNA probe exhibiting minimal background fluorescence. Upon the recognition of specific target miRNA, an ISDPR was triggered to produce numerous massive specific DNA-miRNA duplex helixes, and a strong emission was observed due to the weak interaction between the DNA-miRNA duplex helix and GO. A miRNA biosensor down to 2.1 fM with a linear range of 4 orders of magnitude was obtained. Furthermore, the large planar surface of GO allows simultaneous quenching of several DNA probes with different dyes and produces a multiple biosensing platform with high sensitivity and selectivity, which has promising application in profiling the pattern of miRNA expression and biomedical research.

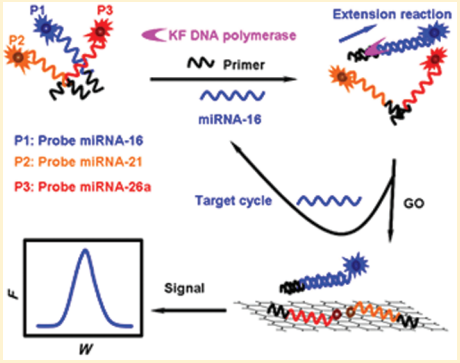

MicroRNA (miRNA) is a group of small endogenous noncoding RNAs (approximately 18−25 nucleotides), which encodes in the genomes of different species.[1−3] MiRNA is associated with an RNA-induced silencing protein complex to partially complement with the 3-untranslated region of target mRNAs in cytoplasm, which further mediate mRNA cleavage or inhibit protein synthesis.[4−6] It plays significant regulatory roles in a diverse range of biological processes such as cell development, differentiation, metabolism, and apoptosis.[7−10] Specifically, aberrant expression of miRNA was found in various cancers.[11,12] Therefore, miRNA is a clinically important class of diagnostic and prognostic markers and is useful in basic biomedical research.[13−15] Current widely used miRNA analysis methods, including the real time reverse transcription polymerase chain reaction,[16] Northern blotting,[17] and miRNA array[18] technology, could meet the detection requirement to some degree. However, miRNA analysis is still challenging, owing to the unique characteristics of miRNA, including short size, sequence similarity among family members, low abundance, and susceptibility to degradation. With these characteristics, the improved profile strategy for rapid, sensitive, and multiple detection of miRNA is an urgent need.[19−22]

The integration of the unique optical, electronic, and catalytic properties of nanomaterials with highly specific recognition ability of biomolecules has been used to develop many new-style tools for bioanalysis.[23,24] For example, a series of gold nanoparticle-based DNA assays have been developed,[25−28] and various carbon nanostructures such as carbon tubes, carbon nanodots, and carbon nanofibers have extensively been used for development of biosensors.[29−32] Recently, graphene oxide (GO), a two-dimensional nanomaterial, has been extensively studied due to its unique and excellent electronic, thermal, and mechanical properties. Specifically, the extraordinary and distance-dependent fluorescence quenching property of GO has been employed to elaborately design sensors for diverse biomolecules in homogeneous solution.[33−35] For example, the quenching effect has provided a biosensing platform for the detection of DNA based on the conformation alteration of dye-labeled DNA for its release from the GO upon the recognition binding with target sequence.[33] A graphene nanoprobe was used for rapid, sensitive, and multicolor fluorescent DNA

Received: March 14, 2012
Accepted: April 17, 2012
Published: April 17, 2012

   dx.doi.org/10.1021/ac300721u | *Anal. Chem.* 2012, 84, 4587−4593

analysis by Fan and co-workers.[34] Our group also proposed an effective sensing platform for detecting biomolecules, based on the fluorescence resonance energy transfer from quantum dots to GO.[35] However, detection of biomolecules with high sensitivity remains a great challenge, and the low abundance of these biomolecules limits the broad application of these GO-based methods.

This work proposed a rapid, sensitive, selective multiple miRNA detection assay by coupling the GO distance-dependent florescence quenching with isothermal strand-displacement polymerase reaction (ISDPR) for improving sensitivity (Scheme 1). In the absence of specific targets,

Scheme 1. Illustration of the GO Fluorescence Quenching and ISDPR-Based Multiple miRNA Analysis

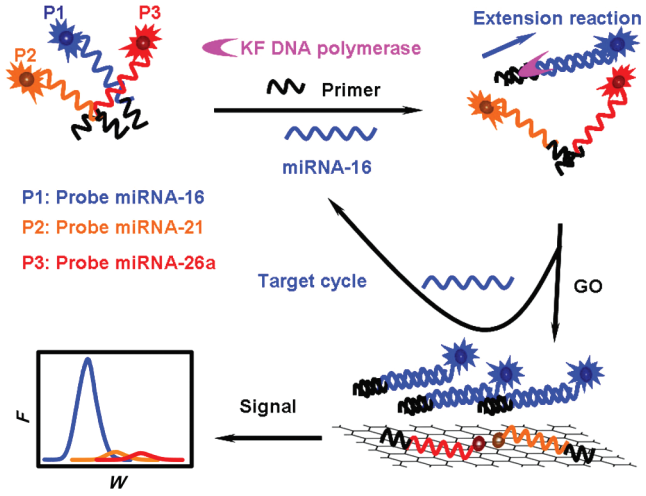

ISDPR could be triggered for neither P2 nor P3 due to weak duplex stability arising from the low melting temperature (Tm) of P and probes (P2, P3). The high fluorescent quenching efficiency of GO by a FRET-based mechanism in combination with strong interaction between ssDNA and GO made the ssDNA P2, P3 labeled with fluorescent dye exhibit minimal background fluorescence. Given the presence of the specific target (T1), upon the corresponding P1 recognizing the target, the Tm of P1 and P would increase by several degrees due to the adjacent base stacking and forming a stable duplex structure. An ISDPR producing numerous massive DNA-miRNA duplex helixes could be triggered in the presence of four nucleotides (dNTPs) and Klenow fragment exo$^-$ (KF) DNA polymerase. A strong fluorescent emission was observed for the fluorescence of P1 due to the weaker interaction between the DNA-miRNA duplex helix and GO. The high signal-to-background ratio and ISDPR-based target amplification produced a miRNA biosensor with high sensitivity, and the large planar surface of GO made it possible to simultaneously quench several DNA probes with different dyes and obtain a multiple biosensing platform for the detection of different miRNA targets in the same solution.

EXPERIMENTAL SECTION

Materials and Reagents. Graphite powder and sodium borohydride of analytical grade were obtained from Sinopharm Chemical Reagent Co. Ltd. (China). dNTPs and KF DNA polymerase were obtained from Fermentas (Lithuania). DNA hybridization buffer (HB) was phosphate-buffered saline (137 mM NaCl, 2.5 mM Mg^{2+}, 10 mM Na_2HPO_4, and 2.0 mM KH_2PO_4, pH 7.4). DNA was stored in Tris-HCl (10 mM, pH 8.0) containing 1 mM ethylenediaminetetraacetic acid. Ultrapure water obtained from a Millipore water purification system (≥18 MΩ, Milli-Q, Millipore) and was used in all runs. All other reagents were of analytical grade. The oligonucleotides were purchased from Sangon Biological Engineering Technology & Co. Ltd. (Shanghai, China) and purified using high-performance liquid chromatography. Their sequences were (1) primer (P), 5′-**CACACAGA**-3′; (2) probe miRNA-16 (P1), 5′-carboxy fluorescein (FAM)-CGC CAA TAT TTA CGT GCT GCT **ATC TGT GTG**-3′; (3) probe miRNA-21(P2): 5′-6-carboxy-x-rhodamine (ROX)-TCA ACA TCA GTC TGA TAA GCT **ATC TGT GTG**-3′; (4) probe miRNA-26a (P3), 5′-cyanine dye 5 (Cy 5)-AGC CTA TCC TGG ATT ACT TGA **ATC TGT GTG**-3′.

All the RNA sequences were purchased from Shanghai GenePharma Co., Ltd. (Shanghai, China): (1) miRNA-16 (T1), UAGCAGCACGUAAAUAUUGGCG; (2) miRNA-21 (T2), UAGCUUAUCAGACUGAUGUUGA; (3) miRNA-26a (T3), U UCA AGU AAU CCA GGAUAGGCU; (4) probe miRNA-16 complement band (T4), **CAC ACA GA**U AGC AGC ACG UAA AUA UUG GCG; (5) single-base mismatch stand of miRNA-16 (T5), UAGCAGCAC-GUAAAUAUUGCCG; (6) three-base mismatch stand of miRNA-16 (T6), UAACAGCACGAAAAUAUUGCCG.

Instruments. The morphologies of GO were examined with an Agilent 5500 atomic force microscopy (AFM) and a JEM 2100 transmission electron microscope (TEM). AFM measurements were carried out on Nanoscope IIIa (Digital Instrument) under tapping mode. A droplet of GO dispersion was cast onto a freshly cleaved mica surface, and the sample was kept at room temperature to allow water evaporation for obtaining the sample. The image was obtained at room temperature (25 °C) with a humidity of 30%. All fluorescence spectra were collected with a Hitachi F-4500 spectrophotometer equipped with a xenon lamp excitation source. The Fourier transform-infrared spectroscopic (FT-IR) spectrum was measured on a Nicolet 400 Fourier transform-infrared spectrometer (Madison, WI). The Raman spectrum was recorded with a Renishaw-inVia Raman microscope (Renishaw, United Kingdom).

Synthesis of Graphene Oxide. GO was produced from graphitic powder according to Hummer's method with some modification.[36,37] Briefly, graphite powder (3 g) was added into a solution consisting of concentrated H_2SO_4 (12 mL), $K_2S_2O_8$ (2.5 g), and P_2O_5 (2.5 g) and reacted for 4.5 h at 80 °C. The resulting mixture was then diluted with 0.5 L of water and kept at 80 °C for another 12 h. The residual acid was removed by filtrating and washing with water, and the obtained reagent was dried under ambient conditions overnight. The reagent was further oxidized in concentrated H_2SO_4 (120 mL) containing $KMnO_4$ (15 g), which was added gradually under stirring, while keeping the temperature less than 20 °C. This mixture was stirred at 40 °C for 30 min and then 90 °C for 90 min. Afterward, the mixture was diluted with water (250 mL) and kept at 105 °C for 25 min. The resulting mixture was stirred for 2 h; 0.7 L of water and 20 mL of 30% H_2O_2 were then added to end the reaction. The mixture was purified by filtration and washed with 1:10 HCl aqueous solution and water several times. Finally, the product was further purified by dialysis for 1 week to remove the remaining metal species.

Fluorescent miRNA assays. In a typical miRNA assay, the P1 (probe miRNA-16) (1 μL, 1 μM) was mixed with primer (1

dx.doi.org/10.1021/ac300721u | Anal. Chem. 2012, 84, 4587−4593

μL, 1 μM) and target miRNA-16 at different concentrations (1 μL) in 10 μL of reaction buffer (50 mM, pH 7.5 Tris-HCl buffer, 10 mM magnesium acetate, 33 mM potassium acetate, 1 mM dithiothreitol, 10 mM dNTP, and 0.1% Tween 20) containing 0.2 units of KF DNA polymerase at 25 °C for 1 h to perform the ISDPR reaction, then kept at 70 °C for 10 min to end the reaction. After the mixture was diluted with 186 μL of HB (137 mM NaCl, 2.5 mM Mg^{2+}, 10 mM Na_2HPO_4, and 2.0 mM KH_2PO_4, pH 7.4), GO (1 μL, 0.2 mg/mL) was added. After 10 min of incubation, fluorescence measurements were carried out to monitor the hybridization process.

Several MiRNAs Analysis. For several miRNA analysis, the solution containing P1 (1 μL, 1 μM), P2 (1 μL, 1 μM), P3 (1 μL, 1 μM), and P (3 μL, 1 μM) was mixed with target miRNA-16 (1 μL), miRNA-21 (1 μL), or miRNA-26a (1 μL) at different concentrations in 10 μL of reaction buffer (50 mM, pH 7.5 Tris-HCl buffer, 10 mM magnesium acetate, 33 mM potassium acetate, 1 mM dithiothreitol, 10 mM dNTP, and 0.1% Tween 20) containing 0.2 units of KF DNA polymerase at 25 °C for 1 h to perform the ISDPR reaction. After the mixture was diluted with 184 μL of HB (137 mM NaCl, 2.5 mM Mg^{2+}, 10 mM Na_2HPO_4, and 2.0 mM KH_2PO_4, pH 7.4), GO (1 μL, 0.2 mg/mL) was added. After 10 min incubation, fluorescence measurements were carried out to analyze the hybridization process.

RESULTS AND DISCUSSION

Characterization of GO. GO prepared according to Hummers method displays high water-solubility due to the massive suspended hydroxyl and carboxyl group present at the surface,[36,37] so we first characterized the exfoliation of the GO. Figure 1A is a typical tapping mode AFM image of the as-prepared GO, which simultaneously collects height and size-distributed data of GO. The cross-sectional view of the AFM image shows that the resulting GO is almost a single layer with an average thickness of about 0.919 nm, agreeing with some previous reports attributing ~1.0 nm thick GO to a single layer.[38,39] The size distribution of GO was within a narrow range from 70 to 400 nm in lateral width. The cross-sectional view of the typical TEM image of as-prepared GO shows that the single layer GO sheet exhibits a size about 350 nm in lateral width, and occasional folds, crinkles, and rolled edges are also observed (Figure 1B). The single layer GO sheet with relative narrow size distribution is useful for homogeneous analysis. The FT-IR and Raman spectrum of GO were further examined to prove the successful synthesis of GO. The FT-IR spectrum exhibited the characteristic vibrations of GO (Figure 1C), including a broad and intense peak of the O−H group at 3433 cm^{-1}, a O−H deformation peak at 1418 cm^{-1}, a C−OH stretching peak at 1260 cm^{-1}, a C−O stretching peak at 1032 cm^{-1}, and a peak at 1627 cm^{-1} attributed to the vibrations of unoxidized graphitic skeletal domains and the adsorbed water molecules.[37] As shown in Figure 1D, the G bands at 1580 cm^{-1} were assigned to the vibration of sp^2 bonded carbon atoms, meanwhile, the Raman spectrum of GO showed the well-documented D at 1350 cm^{-1} assigned to the vibration of carbon atoms with dangling bonds in plane terminations of disordered graphite, indicating the formation of sp^3 carbon in GO.[40]

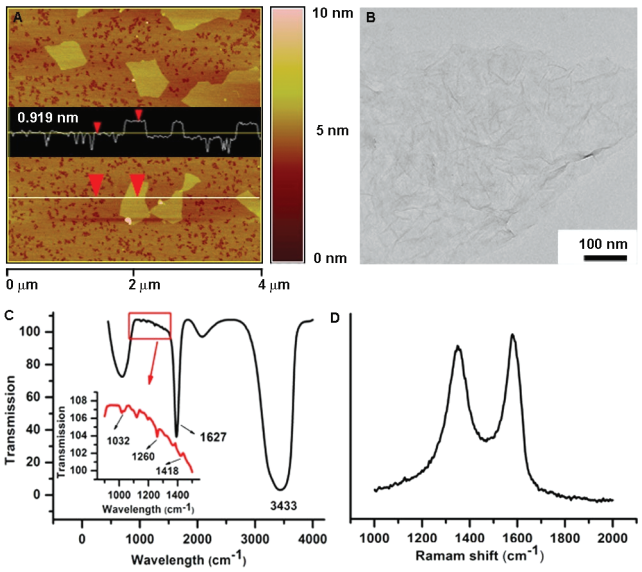

Figure 1. Tapping mode AFM image of GO sheets deposited on mica substrate (A). TEM image of GO sheet (B). FT- IR spectrum (C) and Raman spectrum (D) of as-prepared GO.

GO Fluorescence Quenching Reaction. To investigate the fluorescence quenching ability of GO, the photoluminescence (PL) of GO resulted from the introduction of the bandgap[41,42] was first investigated under the excitation wavelength from 450 to 700 nm. As shown in Figure 2, no obvious PL peak was observed in the wavelength range, indicating the effective excitation wavelength of the PL was not in the range and the interference to fluorescence detection from the PL of GO is negligible. The fluorescence change of FAM tagged on ssDNA of miRNA-16 probe caused by GO was then examined. It was found that the fluorescence of the FAM-tagged miRNA-16 probe was rapidly quenched by GO, and the fluorescence quenching depended on the ratio of miRNA-16 probe to GO. The fluorescence of FAM of miRNA-16 probe (5 nM) was almost completely quenched by GO (1.2 μg/mL) (Figure 3A), indicating excellent fluorescent quenching of GO. Fluorescence measurement was performed to study the difference of fluorescence quenching kinetics of organic dye labeled on the ssDNA and ssDNA hybridized with its miRNA

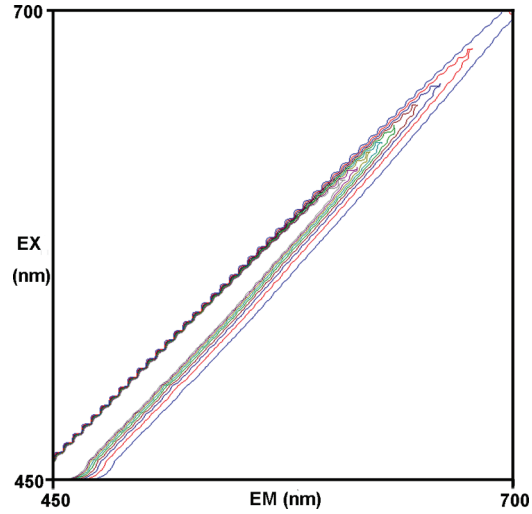

Figure 2. Contour map of fluorescence from GO solution (1 μg/mL). Central blank regions along $\lambda_{ex} = \lambda_{em}$, scattered light prevent detection of fluorescence.

dx.doi.org/10.1021/ac300721u | Anal. Chem. 2012, 84, 4587−4593

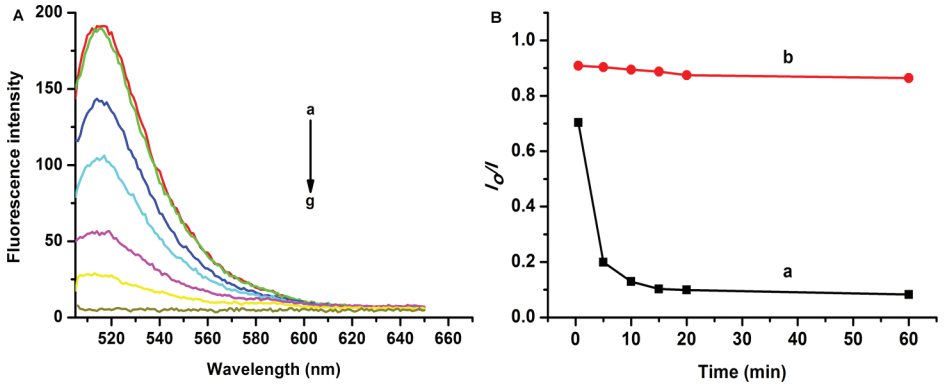

Figure 3. (A) Fluorescence quenching of FAM labeled on ssDNA (5 nM) in the presence of GO with a series of concentrations (a–g) 0.1, 0.2, 0.4, 0.6, 0.6, 0.8, 1.0, and 1.2 μg/mL). (B). Fluorescence quenching of P1 (5 nM) in HB buffer (a) and P1 incubated with target (5 nM) (b) by GO (1 μg/mL) as a function of time. Fluorescence intensity was recorded at 515 nm with an excitation wavelength of 490 nm.

target by GO. As shown in Figure 3B, upon addition of GO (1 μL, 0.2 mg/mL) into the P1 (200 μL, 5 nM) solution, fluorescence intensity of P1 decreased rapidly to 12% of the original intensity in 10 min (Figure 3B, curve a), which indicated the strong and fast quenching effect of GO on the fluorescence of FAM tagged on ssDNA. Nevertheless, when P1 hybridized with its complement strand (T4, 5 nM) at the same concentration and formed a DNA-RNA duplex helix, the FAM showed a slow decrease in the intensity (Figure 3B, curve b) and the fluorescence intensity remained at 86% of the original intensity 1 h later. The quenching phenomenon arose from the long-range energy transfer mechanism from the dye to the GO in a distant-dependent pattern. For the fluorescent ssDNA probe, it could be rapidly adsorbed on GO due to the interaction between GO and the base of the ssDNA as well as the hydrogen bonding interaction present between −OH or −COOH groups of GO and −OH or $-NH_2$ groups of the ssDNA.[43] Its fluorescence could be efficiently quenched by the GO. After forming a DNA-RNA duplex helix, the interaction between the GO and the duplex helix became weaker, resulting in the dye being kept away from the GO and a strong fluorescence.

Figure 4 shows the fluorescence quenching of P1 hybridized with T4, mixture of T1 and P, T1, P, and no target by GO (curve a–e), respectively. The I_0/I value for P1 hybridized with

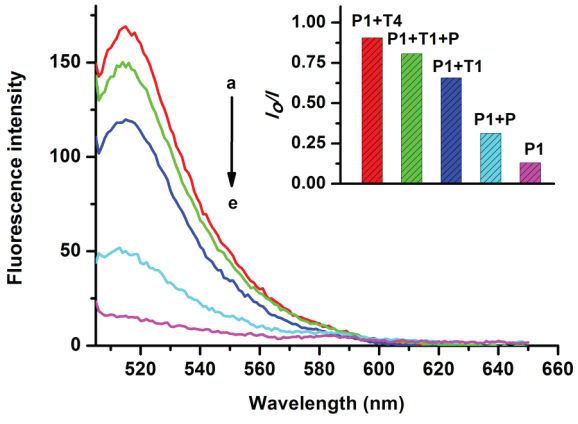

Figure 4. Fluorescence quenching of P1 (5 nM) by GO (1 μg/mL) in HB buffer incubated with different strands (a–e) T4, mixture of T1 and P, T1, P, and no target (5 nM). Inset: I_0/I ratio for six cases upon addition of GO with different concentrations.

P, T1, P, and T1, T4 was 1.68-fold, 3.5-fold, 4.3-fold, and 4.8-fold of the value of P1 (Figure 4, inset), the fluorescence of which was efficiently quenched by GO (1.0 μg/mL) due to the long-range energy transfer from the dye to the GO and strong interaction between GO and ssDNA. In this manner, I and I_0 are the fluorescence intensities of P1 hybridized with different strands (5 nM) in the absence and presence of GO at 515 nm, respectively. The results indicated more single sequence regions, along with more fluorescence quenching. The difference in quenching efficiencies between the organic dye labeled on ssDNA and the ssDNA forming a DNA-miRNA duplex helix by GO produced a potential platform for sensing target miRNA.

ISDPR. Duplex stability is affected by sequence composition, strand length, ionic strength, and temperature,[44] while base pairing and stacking between adjacent bases are two essential parameters that contribute to the major forces.[45] The Tm of P1 and the P increases by several degrees in the presence of an adjacent T1; thus, there is an increase in the stability of the duplex formed.[46] In this proposed method, appropriate temperature must be selected to meet the requirement that efficiently triggers ISDPR in the presence of the target, while not triggering any ISDPR in the absence of target to reduce the false positive signal. The fluorescence quenching degree of ISDPR products by GO is inversely correlated with the ISDPR efficiency, due to the weak interaction between the forming DNA-RNA duplex helix and GO. The dye was kept away from the GO and resulted in a strong fluorescence. Therefore, the ISDPR of the mixture containing P1 and P in the absence and presence of T1 were carried out in different temperatures, and fluorescence quenching of the corresponding products by GO was investigated. Figure 5 shows the fluorescence quenching reaction of the obtained ISDPR products of the two systems by GO. It was found that both the mixture containing P1 and P in absence and presence of T1 can efficiently trigger the ISDPR when the temperature is less than 30 °C. When the temperature was further increased to 35 °C, the fluorescence quenching sharply increased for the cases in the absence of T1, indicating P could not efficiently hybridize with the P1 and trigger ISDPR at this temperature and the higher temperatures without the target due to the weak duplex stability. The decrease of ISDPR efficiency was also observed for the mixture in the presence of T1, which might have arose from the integration of decrease in enzyme activity and stability of the duplex helix. The maximized signal-to-background ratio was

dx.doi.org/10.1021/ac300721u | *Anal. Chem.* 2012, 84, 4587–4593

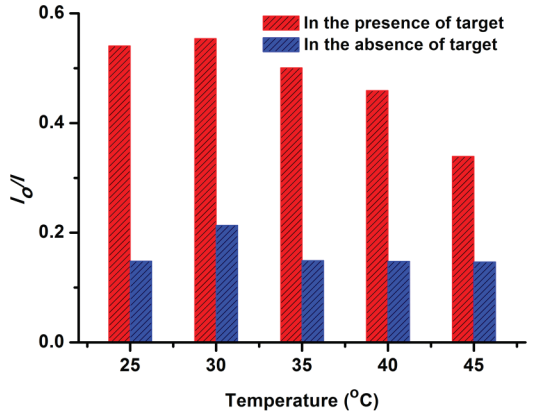

Figure 5. Fluorescence quenching by GO (1 μg/mL) of a mixture containing P1 (5 nM) and P (5 nM) in the presence (red histogram) and absence (blue histogram) of T1 (5 pM) and triggering ISDRR at different temperatures (25–45 °C).

obtained at 25 °C; thus, the temperature of 25 °C was used in the subsequent work.

Fluorescent miRNA Assays. The bottleneck of the GO-based or other analogical homogeneous detection approach is the relatively lower sensitivity compared to other methods,[47−49] and the limit of detection (LOD) of the GO-based method is always at the nanomolar level. Given the emerging diagnostic value of miRNA, it is significant that the detection methods need to be simple and highly sensitive. In this regard, we introduced the ISDPR into the GO-based detection to improve the sensitivity. With the increasing concentration of T1 used for hybridization in the mixture containing P1 and P, the fluorescence emission intensity increased in the presence of the GO (Figure 6). The plot of the fluorescence intensity ratio

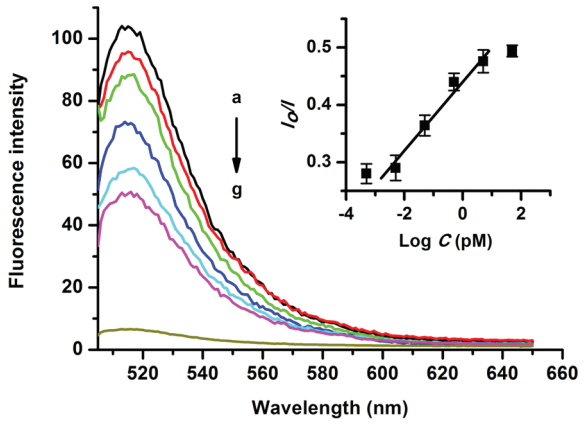

Figure 6. Fluorescence emission spectra of P1 (5 nM) after incubation with 50, 5, and 0.5 pM and 50, 5, 0.5, and 0 fM target (a–g), ISDPR, and then addition of GO (1 μg/mL) for 10 min. Inset: plot of fluorescent intensity ratio I_0/I vs logarithm of target concentration.

I_0/I vs the logarithm value of T1 concentration displayed a linear relationship in the range from 5 pM to 5 fM (Figure 6, inset). The LOD for target T1 was 2.1 fM at 4 times the standard deviation of the control (free of target T1). This LOD of 2.1 fM was much lower than the GO-based postmixing DNA detection system with a LOD of 10 nM[33] and was also lower than the GO-based premixing DNA detection system with a LOD of 100 pM.[34] This method was also superior to some other homogeneous detection methods such as molecular beacons,[50] gold nanoparticle-DNA-dye conjugates,[51] SWNT-based DNA detection,[52] and the silver nanocluster-based miRNA detection.[53] Meanwhile, the LOD was competitive with other sensitive miRNA detection strategies such as surface plasmon resonance,[54] nanocrystals-based fluorescence detection,[55] and electrochemical detection.[56] The GO-based detection strategy involving ISDPR exhibited high signal-to-noise ratio and high sensitivity due to the hybridization event that was related to massive ISDPR products.

The selectivity of the proposed system was investigated by three kinds of DNA sequences with the same concentration (5 pM) including T1 (complementary target), T5 (single-base mismatched strand), and T6 (three-base mismatched strand). As shown in Figure 7, the proposed system displayed high

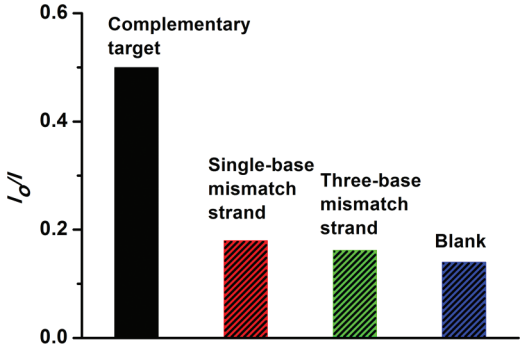

Figure 7. Fluorescent intensity ratio I_0/I of P1 (5 nM) after incubation with complementary target (5 pM), single-base mismatch strand (5 pM), three-base mismatch strand (5 pM), and no target, ISDPR, and then addition of GO (1 μg/mL) for 10 min.

sequence specificity to discriminate the perfectly complementary target and the mismatched strands. The perfectly complementary target showed a I_0/I value of 2.78 times that for single-base mismatch sequence, and the response to a three-base mismatch strand was only 32% of that for the perfectly complementary target, which was almost equal to the blank control with a I_0/I value of 28% of that for the perfectly complementary target. The high sequence specificity may be attributed to the competition between GO/probe adsorption and probe target hybridization.[30] These results suggested that the proposed miRNA detection approach was high sequence specificity and had potential application in single nucleotide polymorphism analysis.

MiRNA Analysis. Simultaneous detection of multiple miRNA opens new opportunities for understanding the miRNA expression pattern for disease molecular diagnosis and new drug discovery. It is therefore critical to develop robust, sensitive, and simple detection methods for multiple miRNA analysis. The large planar surface and excellent multiple organic dye fluorescence quickening of GO allows it to interact with several DNA strands simultaneously and detect miRNA targets in the same solution (Scheme 1). Three probes (P1, P2, and P3) labeled with FAM, Cy5, and ROX were designed, respectively, and their performance in several miRNA detection was evaluated by fluorescence measurement. As shown in Figure 8, after the addition of specific miRNA targets to the probe mixture containing P, P1, P2, and P3 and subsequent ISDPR and addition of GO, a strong emission only from the corresponding wavelength could be observed (Figure 8A). For example, the addition of the T1 just produced the specific fluorescent emission of the blue FAM (Figure 8A, column a).

dx.doi.org/10.1021/ac300721u | Anal. Chem. 2012, 84, 4587−4593

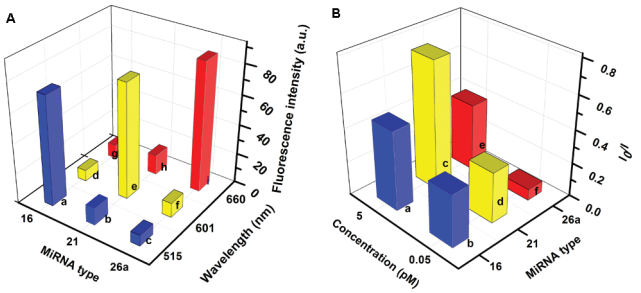

Figure 8. (A) Fluorescence intensity of P1 (columns a,b,c), P2 (columns d,e,f), P3 (columns g,h,i) in the presence of different targets (5 pM), followed by ISDPR and addition of GO (1 μg/mL) for 10 min, respectively. (B) I/I_0 values of P1 (columns a,b), P2 (columns c,d), and P3 (columns e,f) at different concentrations of target: 5 pM (columns a,c,e) and 0.05 pM (columns b,d,f).

Minimal emission of blue FAM was observed when T2 or T3 with same concentration was added in the similar process, which exhibited 15.5% and 11%, respectively, fluorescence intensity of the blue FAM (Figure 8A, column b,c) for the T1 case. Similarly, T2 and the T3 caused a strong fluorescence emission from the orange ROX color (Figure 8A, column e), and red Cy5 color (Figure 8A, column i), respectively, with minimal emission when added to the other targets.

Furthermore, it was discovered that the corresponding fluorescence intensity decreased along with the concentration decrease of the specific target in the mixture containing P, P1, P2, and P3 (Figure 8B). Columns a and b are the I_0/I values of FAM-labeled P1 in the probes mixture incubated with T1 at different concentrations of 5 and 0.05 pM, respectively, followed by ISDPR and addition of GO to the solution. The I_0/I value decreased from 0.47 to 0.31, when the concentration of T1 decreased from 5 to 0.05 pM. The result showed a higher target concentration along with more ineffective fluorescence quenching. A similar experiment result was observed for the T2 (columns c,d) and the T3 (columns e,f). These results indicated GO fluorescence quenching and ISDPR-based target amplification provide a promising approach for multiple miRNA analysis. Meanwhile, the high signal-to-noise ratio and the sequence specificity facilitated the proposed GO-based miRNA detection method profiling multiple miRNAs with high specificity.

CONCLUSIONS

There is an urgent need for developing robust, highly sensitive, selective multiple miRNAs detection methods due to its potential application in disease molecular diagnoses and biomedicine. Here, we proposed a simple, highly sensitive, selective multiple miRNAs detection methods based on the ISDPR and GO fluorescence quenching. The capability of GO to discriminate ssDNA and double-stranded nucleic acid structure (DNA/DNA or DNA/RNA) in combination with the excellent organic fluorescence quenching of GO allows the proposed strategy to detect miRNA in the same solution with high selectivity, while the ISDPR-based target amplification endows the detection method with high sensitivity. Meanwhile, the large planar surface of GO makes it possible to simultaneously quench several DNA probes with different dyes, producing a multiple biosensing platform for the detection of different miRNA targets in the same solution. The proposed strategy provides a reliable, simple, highly sensitive, and selective multiple miRNA detection method and shows promising application in molecular disease diagnosis and biomedicine.

AUTHOR INFORMATION

Corresponding Author

*Huangxian Ju: phone/fax, +86-25-83593593; e-mail, hxju@nju.edu.cn. Xueji Zhang: phone/fax, +86 10 82376993; e-mail, zhangxueji@ustb.edu.cn.

Notes

The authors declare no competing financial interest.

ACKNOWLEDGMENTS

The authors wish it to be known that, in their opinion, the first two authors should be regarded as joint first authors. This work was funded by China Postdoctoral Science Foundation (NO. 11175012), the Chinese Central Universities Funds (NO. FRF-TP-12-171A, NO. 06108037, 06199019, 06108101), the National Natural Science Foundation of China (Grants NO. 21127007, 21075055, 21135002, and 21121091) and the National Research Program of China (Grant 2010CB732400).

REFERENCES

(1) Grishok, A.; Pasquinelli, A. E.; Conte, D.; Li, N.; Parrish, S.; Ha, I.; Baillie, D. L.; Fire, A.; Ruvkun, G.; Mello, C. C. *Cell* **2001**, *106*, 23−24.
(2) Mallory, A. C.; Vaucheret, H. *Nat. Genet.* **2006**, *38* (Suppl1), S31−S36.
(3) Cullen, B. R. *Nat. Genet.* **2006**, *38* (Suppl 1), S25−S30.
(4) Cao, X.; Yeo, G.; Muotri, A. R.; Kuwabara, T.; Gag, F. H. *Annu. Rev. Neurosci.* **2006**, *229*, 77−103.
(5) Bartel, D. P. *Cell* **2004**, *116*, 281−297.
(6) Ambros, V. *Nature* **2004**, *431*, 350−355.
(7) Plasterk, R. H. *Cell* **2006**, *124*, 877−881.
(8) Joglekar, M. V.; Joglekar, V. M.; Hardikar, A. A. *Gene Expression Patterns* **2009**, *9*, 109−113.
(9) Xu, P.; Vernooy, S. Y.; Guo, M.; Hay, B. A. *Curr. Biol.* **2003**, *13*, 790−795.
(10) Brennecke, J.; Hipfner, D. R.; Stark, A.; Russell, R. B.; Cohen, S. M. *Cell* **2003**, *113*, 25−36.
(11) Jiang, J.; Lee, E. J.; Gusev, Y.; Schmittgen, T. D. *Nucleic Acids Res.* **2005**, *33*, 5394−5403.
(12) Wark, A. W.; Lee, H. J.; Corn, R. M. *Angew. Chem., Int. Ed.* **2008**, *47*, 644−652.
(13) Barbarotto., E.; Schmittgen, T. D.; Calin, G. A. *Int. J. Cancer* **2008**, *122*, 969−977.
(14) Kumar, M. S.; Lu, J.; Mercer, K. L.; Golub, T. R.; Jacks, T. *Nat. Genet.* **2007**, *39*, 673−677.
(15) Gupta, A.; Gartner, J. J.; Sethupathy, P.; Hatzigeorgiou, A. G.; Fraser, N. W. *Nature* **2006**, *442*, 82−85.
(16) Li, J.; Yao, B.; Huang, H.; Wang, Z.; Sun, C. H.; Fan, Y.; Chang, Q.; Li, S. L.; Wang, X.; Xi, J. Z. *Anal. Chem.* **2009**, *81*, 5446−5451.
(17) Pall, G. S.; Codony-Servat, C; Byrne, C. J.; Ritchie, L.; Hamilton, A. *Nucleic Acids Res.* **2007**, *35*, e60.
(18) Nelson, P. T.; Baldwin, D. A.; Scearce, L. M.; Oberholtzer, J. C.; Tobias, J. W.; Mourelatos, Z. *Nat. Methods* **2004**, *1*, 155−161.
(19) Arefian, E.; Kiani, J.; Soleimani, M.; Shariati, S.; Ali., M.; Aghaee-Bakhtiari, S. H.; Atashi, A.; Gheisari, Y.; Ahmadbeigi, N.; Banaei-Moghaddam, Ali. M.; Naderi, M.; Namvaras, N.; Good, L.; Faridani, Omid. R. *Nucleic Acids Res.* **2011**, *39*, e80.
(20) Pöhlmann, C.; Sprinzl, M. *Anal. Chem.* **2010**, *82*, 4434−4440.
(21) Valoczi, A.; Hornyik, C.; Varga, N.; Burgyan, J.; Kauppinen, S.; Havelda, Z. *Nucleic Acids Res.* **2004**, *32*, e175.
(22) Zhang, Y.; Zhang, C. Y. *Anal. Chem.* **2012**, *84*, 224−231.
(23) Yang, H.; Xia, Y. *Adv. Mater.* **2007**, *19*, 3085−3087.
(24) Solanki1, P. R.; Kaushik1, A.; Agrawal, V. V.; Malhotra1., B. D. *PG Asia Mater.* **2011**, *3*, 17−24.

(25) Elghanian, R.; Storhoff, J. J.; Mucic, R. C.; Letsinger, R. L.; Mirkin, C. A. *Science* **1997**, *277*, 1078−1080.
(26) Rosi, N. L.; Mirkin, C. A. *Chem. Rev.* **2005**, *105*, 1547−1562.
(27) Li, H.; Rothberg, L. *Proc. Natl. Acad. Sci. U.S.A.* **2004**, *101*, 14036−14039.
(28) Han, M. S.; Lytton-Jean, A. K. R.; Oh, B. K.; Heo, J.; Mirkin, C. A. *Angew. Chem., Int. Ed.* **2006**, *118*, 1839−1842.
(29) Cheng, W.; Ding, L.; Lei, J. P.; Ding, S. J.; Ju, H. X. *Anal. Chem.* **2008**, *80*, 3867−3872.
(30) Fu, C. C.; Lee, H. Y.; Chen, K.; Lim, T. S.; Wu, H. Y.; Lin, P. K.; Wei, P. K.; Tsao, P. H.; Chang, H. C.; Fann, W. *Proc. Natl. Acad. Sci. U.S.A.* **2007**, *104*, 727−732.
(31) Hao, C.; Ding, L.; Zhang, X. J.; Ju, H. X. *Anal. Chem.* **2007**, *79*, 4442−4447.
(32) Yang, R. H.; Jin, J. Y.; Chen, Y.; Shao, N.; Kang, H. Z.; Xiao, Z. Y.; Tang, Z. W.; Wu, Y. R.; Zhu, Z.; Tan, W. H. *J. Am. Chem. Soc.* **2008**, *130*, 8351−8358.
(33) Lu, C. H.; Yang, H. H.; Zhu, C. L.; Chen, X.; Chen, G. N. *Angew. Chem., Int. Ed.* **2009**, *48*, 4785−4787.
(34) He, S. J.; Song, B.; Li, D.; Zhu, C. F.; Qi, W. P.; Wen, Y. Q.; Wang, L. H.; Song, S. P.; Fang, H. P.; Fan, C. H. *Adv. Funct. Mater.* **2010**, *20*, 453−459.
(35) Dong, H. F.; Gao, W. C.; Yan, F.; Ji, H. X.; Ju, H. X. *Anal. Chem.* **2010**, *82*, 5511−5517.
(36) Hummers, W. S.; Offeman, R. E. *J. Am. Chem. Soc.* **1958**, *80*, 1339−1339.
(37) Xu, Y. X.; Bai, H.; Lu, G. W.; Li, C.; Shi, G. Q. *J. Am. Chem. Soc.* **2008**, *130*, 5856−5857.
(38) Li, X.; Wang, X.; Zhang, L.; Lee, S.; Dai, H. *Science* **2008**, *319*, 1229−1232.
(39) Stankovich, S.; Dikin, D. A.; Dommett, G. H. B.; Kohlhaas, K. M.; Zimney, E. J.; Stach, E. A.; Piner, R. D.; Nguyen, S. T.; Ruoff, R. S. *Nature* **2006**, *442*, 282−286.
(40) Shen, J. F.; Hu, Y. Z.; Shi, M.; Lu, X.; Qin, C.; Li, C.; Ye, M. G. *Chem. Mater.* **2009**, *21*, 3514−3520.
(41) Nourbakhsh, A.; Cantoro, M.; Vosch,T.; Pourtois, G.; Clemente, F.; Veen, M. H. V. D.; Hofkens, J.; Heyns, M. M.; Gendt, S. D.; Sels B. F. *Nanotechnology* **2010**, *21* 435203.
(42) Nourbakhsh, A.; Cantoro, M.; Klekachev, A. V.; Pourtois, G.; Vosch, T.; Hofkens, J.; Veen, M. H. V. D.; Heyns, M. M.; Gendt, S. D.; Sels, B. F. *J. Phys. Chem. C* **2011**, *115*, 16619−16624.
(43) Yang, X.; Zhang, X.; Liu, Z.; Ma, Y.; Huang, Y.; Chen, Y. *J. Phys. Chem. C* **2008**, *112*, 17554−17558.
(44) Wetmur, J. G. *Annu. Rev. Biophys. Bioeng.* **1976**, *5*, 337−361.
(45) Kool, E. T. *Annu. Rev. Biophys. Biomol. Struct.* **2001**, *30*, 1−22.
(46) Cai, S.; Lau, C.; Lu., J. Z. *Anal. Chem.* **2010**, *82*, 7178−7184.
(47) Valoczi, A.; Hornyik, C.; Varga, N.; Burgyan, J.; Kauppinen, S.; Havelda, Z. *Nucleic Acids Res.* **2004**, *32*, e175.
(48) Benes, V.; Castoldi, M. *Methods* **2010**, *50*, 244−249.
(49) Thomson, J. M.; Parker, J.; Perou, C. M.; Hammond, S. M. *Nat. Methods* **2004**, *1*, 47−53.
(50) Tyagi, S.; Kramer, F. R. *Nat. Biotechnol.* **1996**, *14*, 303−308.
(51) Dubertret, B.; Calame, M.; Libchaber, A. J. *Nat. Biotechnol.* **2001**, *19*, 365−370.
(52) Liu, Y; Wang, Y. X.; Jin, J. Y.; Wang, H; Yang, R. H.; Tan, W. H. *Chem. Commun.* **2009**, *6*, 665−667.
(53) Yang, S. W.; Vosch, T. *Anal. Chem.* **2011**, *83*, 6935−6939.
(54) Qavi, A. J.; Kindt, J. T.; Gleeson, M. A.; Bailey, R. C. *Anal. Chem.* **2011**, *83*, 5949−5956.
(55) Li, J. S.; Schachermeyer, S.; Wang, Y.; Yin, Y. D.; Zhong, W. W. *Anal. Chem.* **2009**, *81*, 9723−9729.
(56) Gao, Z. Q.; Yang, Z. C. *Anal. Chem.* **2006**, *78*, 1470−1477.